REPORT DOCUMENTATION PAGE

Form Approved
OMB No. 0704-0188

1. REPORT DATE *(DD-MM-YYYY)*	2. REPORT TYPE	3. DATES COVERED *(From - To)*
31-10-2004	Final Report	May 1 2004 - October 31 2004

4. TITLE AND SUBTITLE
Probabilistic Error Estimation in Model-Based Predictions

5a. CONTRACT NUMBER
N00014-04-M-0124

5b. GRANT NUMBER

5c. PROGRAM ELEMENT NUMBER

6. AUTHOR(S)
Nickolas Vlahopoulos

5d. PROJECT NUMBER

5e. TASK NUMBER

5f. WORK UNIT NUMBER

7. PERFORMING ORGANIZATION NAME(S) AND ADDRESS(ES)
Michigan Engineering Services, LLC.
3916 Center Trade Drive
Ann Arbor, MI 48108

8. PERFORMING ORGANIZATION REPORT NUMBER
MES-ONR-SBIR-I-2

9. SPONSORING/MONITORING AGENCY NAME(S) AND ADDRESS(ES)
Office of Naval Research
Dr. Roshdy Barsoum, ONR 334
Ballston Tower One
800 North Quincy Street
Arlington, VA 22217-5660

10. SPONSOR/MONITOR'S ACRONYM(S)
ONR

11. SPONSORING/MONITORING AGENCY REPORT NUMBER

12. DISTRIBUTION AVAILABILITY STATEMENT
Unlimited/Unclassified

13. SUPPLEMENTARY NOTES

14. ABSTRACT
This report was developed under a SBIR contract award for Solicitation topic # N04-137
Modern ship designs can only be successful if the ship can survive in a hostile environment. External threats for a ship can originate from underwater detonations, anti-ship missiles, and even low tech weapons like in the terrorist attack of USS Cole. These threats become even more important as the focal point for naval operations has shifted towards littoral areas, where ships are exposed to a higher risk. Current analysis methods do not provide high level of confidence and large structural design safety factors are used. Thus, ships are heavier and more expensive to construct and maintain than may actually be required. Models that quantify the level of confidence are required in order to provide meaningful and reliable information during the ship design stage. This SBIR project developed a system for probabilistic Error Estimation in model based predictions. It can utilize commercially available non-linear codes for shock analysis (LS-DYNA, ABAQUS, LS-DYNA/USA, etc.) or Navy developed codes (DYSMAS), a limited amount of test data, the level of uncertainty in model parameters and in the test data, in order to update the numerical model for improved probabilistic correlation to the test data. Once the numerical model has been updated, the new development also provides error bounds for the numerical results.

Probabilistic Error Estimation in Model-Based Predictions

SBIR topic N04-137, Final Report 0001AC

Navy Small Business Innovation Research Program

Submitted to: **Office of Naval Research**

Contract Number N00014-04-M-0124

Submitted by:

Michigan Engineering Services, LLC

3916 Trade Center Drive

Ann Arbor, MI 48108

Period covered by this report: May 03, 2004 – October 31, 2004

1. Identification and Significance of the Phase I project

Modern ship designs can only be successful if the ship can survive in a hostile environment. In spite of susceptibility measures (measures to avoid a hit), the importance of vulnerability reduction for warships cannot be emphasized hard enough.[1] Susceptibility measures can never eliminate the probability of a hit with its successive loss of lives, casualties, loss of mission and material. External threats for a ship become even more important as the focal point for naval operations has shifted towards littoral areas, where ships are exposed to an even higher risk.

Engineers are required to make assessments and create new ship designs that will demonstrate high survivability. Unfortunately, current analysis methods do not provide high level of confidence, and instead large structural design safety factors are employed. As a result, ships are heavier and more expensive to construct and maintain than may actually be required. More reliable predictions which can quantify the level of confidence and can incorporate test data for improving the confidence in the predictions are required. Such predictions can support innovative structural configurations in new Navy programs such as the DD(X), and provide lower life-cycle costs with increased survivability.

The LS-DYNA and the ABAQUS commercial codes have been employed for simulating the response of a ship structure to an underwater explosion. The LS-DYNA/USA code is based on boundary elements and simulates the underwater shock fluid-structure interaction based on a doubly asymptotic approximation. It models the interaction of the structure with the surrounding fluid in terms of wet surface variables and it eliminates the need for fluid elements around the outside of the structure. Coupled with LS-DYNA it is used to simulate the response of ships and submarines to shock wave detonation and the bubble gas effects. DYSMAS is a code developed by NSWC/IHD specifically for modeling accurately the damage to naval structures from underwater explosions. This development is based on coupling a hydrocode with a simulation model of the target structure within a parallel computing environment.

Up to date, only deterministic simulations have been performed for the response of ship structures subjected to an explosive detonation. In real ship structures uncertainty exists due to manufacturing variability and imperfections introduced at the welds, due to variations in the materials (i.e. properties of composites, structural damping properties, stiffness properties due to residual stresses from welding, etc.). Uncertainty also originates from the finite element and boundary element modeling practices (i.e. modeling the connections between welded plates, including all the scantlings in the model, etc.) and from capturing accurately the load from the shock and bubble gas effects exerted on the ship hull (i.e. accounting properly for the properties of the mixed phase medium in the vicinity of the ship due to the flow, the effects from the characteristics of the sea-bed, etc.). The results from a deterministic analysis comprise a single realization which may or may not represent accurately the actual behavior of the system which is been modeled. In addition, when deterministic models are employed for design refinement and optimization, the optimum solution typically resides at the boundaries of the feasible region with respect to the constraints. Thus, the uncertainties which exist in the real system can cause the optimized solution to reside in the infeasible domain and lead into a degraded and undesirable performance for the optimum design. In general,

performing design refinement without taking into account uncertainty can be misleading when uncertainties exist in the real physical system which is been modeled.

The work completed during the Phase I effort generated a new capability for updating a numerical model from test data in applications of ship shock analysis due to underwater explosions, and for providing error estimates due to the uncertainty which exists in the ship structures, the modeling techniques, and the loads. The new process is flexible enough in order to utilize limited measurements which may be available for model updating and it considers uncertainty to be present in the test data. ***The end result is an updated model with a higher confidence level in its predictive capabilities. The confidence level associated with the revised simulation model is also part of the final prediction. The new development works with non-linear simulation models and with any variables that an engineer chooses to consider as random.***

The Principal Component Analysis (PCA) [2-4], the Kriging method for metamodel generation [5-8], concepts of validating non-linear finite element models for blast overpressure inside a room from a limited set of test data [9], and principles of modeling uncertainty and predictive accuracy in non-linear finite element models [10] were employed in the new development.

The PCA converts the time histories from the test or from the analysis into "modal" type of information. The term "modal" does not imply that there are any linear limitations. It is utilized as an indication that the time domain histories are decomposed into more fundamental properties. The "modal" information is used for constructing fast running models which are employed by the model update and error estimation procedures. The Kriging method is used to generate metamodels for the principal components of the numerical models and for constructing the fast running models. The generation of the fast running models is essential in performing within a practical amount of time the model updating under uncertainty, and the error estimation, using large finite element models from commercial codes. The Kriging method is also used for enriching the test data if only a limited amount of data is available.

The following list of tasks was completed during the Phase I project. The related technical information is presented in this report:

(i) Metamodel generation.
(ii) Principal Component Analysis (PCA).
(iii) Enrichment of test data.
(iv) Probabilistic model updating.
(v) Error Estimation.
(vi) Case studies:
- Section of generic surface ship
- Barge for which test data and a numerical model were provided by Northrop Grumman Newport News (NN)

During the Phase I effort there was interaction with NN and with NSWC/IHD. The developments of the Phase I project established a solid technical foundation for developments and validation using full scale ship models. Potential topics for a Phase II effort are presented at the end of this report.

2. Technical Developments

2.1 Metamodel generation.

A metamodel (or surrogate model) is comprised by equations that replace the actual simulation model. Metamodels are evaluated from actual simulations performed at a group of sample points. An Optimal Symmetric Latin Hypercube (OSLH) algorithm that offers a combination between computational effort and optimality is utilized for identifying the sample points. Once the sample points and the values for the performance variables are known, the Kriging method is employed for generating one metamodel for each performance function of interest. The Kriging method is based on treating $Z(\tilde{x})$, the error between the actual performance variable $y(\tilde{x})$ and an approximate value β, as a stochastic process:

$$y(\tilde{x}) = \beta + Z(\tilde{x}) \quad (1)$$

where $\tilde{x}$ is the d-dimensional vector of the random variables that defines the point where the performance variable is evaluated, and "d" is the number of random variables. $Z(\tilde{x})$ is considered as a normal process with zero mean and a covariance that can be expressed as:

$$\text{cov}(Z(\tilde{x}_i), Z(\tilde{x}_j)) = \sigma^2 R(\tilde{x}_i, \tilde{x}_j) \quad (2)$$

where σ^2 is the process variance and $R(\tilde{x}_i, \tilde{x}_j)$ is the spatial correlation function (SCF). The equation used for the SCF is:

$$R(\tilde{x}_i, \tilde{x}_j) = \prod_{k=1}^{d} \exp(-\theta_k (x_{i,k} - x_{j,k})^2) \quad (3)$$

and it indicates a process with infinitely differentiable paths in the mean square sense. θ_k is the correlation parameter that corresponds to the k^{th} component of the d-dimensional vector of the random variables $\tilde{x}$, i.e. k=1,2,…,d. For a set $\tilde{x}_s$ comprised by "n" number of sampling points $\tilde{x}_{si}$, i=1,2,…,n

$$\tilde{x}_s^T = \{\tilde{x}_{s1}, \tilde{x}_{s2}, \ldots, \tilde{x}_{sn}\} \quad (4)$$

The corresponding performance variable $\tilde{y}_s$ is considered known and its values are defined as:

$$\tilde{y}_s^T = \{y(\tilde{x}_{s1}), y(\tilde{x}_{s2}), \ldots, y(\tilde{x}_{sn})\} \quad (5)$$

The vector of correlations between the sample points $\tilde{x}_s$ and the evaluation point $\tilde{x}$ can be expressed as:

$$\tilde{r}^T(\tilde{x}) = \{R(\tilde{x}, \tilde{x}_{s1}), R(\tilde{x}, \tilde{x}_{s2}), \ldots, R(\tilde{x}, \tilde{x}_{sn})\} \quad (6)$$

The correlation matrix [R] is also defined among all the sample points:

$$[R] = [R(\tilde{x}_{si}, \tilde{x}_{sj})]_{nxn} \quad (7)$$

The spatial correlation function in Equations (6) and (7) has been defined by Equation (3). In the Kriging method the value of the performance function evaluated by the metamodel at the evaluation point $\tilde{x}$ is treated as a random variable. The computation of β and $Z(\tilde{x})$ in Equation (1) is based on minimizing the mean square error (MSE) in the response

$$MSE[\hat{y}(\tilde{x})] = E[\hat{y}(\tilde{x}) - y(\tilde{x})]^2 \quad (8)$$

subjected to the unbiasedness constraint:

$$E[\hat{y}(\tilde{x})] = E[y(\tilde{x})] \quad (9)$$

Thus, a set of parameters θ_k (k=1,2,…,d) are computed as the solution of minimizing the product $[(\det(R))^{1/n} \cdot \hat{\sigma}^2]$,

Where $\hat{\sigma}^2 = \frac{1}{n}(\tilde{y}_s - \tilde{F}\hat{\beta})^T R^{-1}(\tilde{y}_s - \tilde{F}\hat{\beta})$ (10)

$\tilde{F}$ is a vector of n-dimension with all unit entries and $\hat{\beta}$ defined as:

$$\hat{\beta} = (\tilde{F}^T R^{-1} \tilde{F})^{-1} \tilde{F}^T R^{-1} \tilde{y}_s \quad (11)$$

Once the set of optimal parameters θ_k has been computed, then the performance function at any point $\tilde{x}$ can be evaluated as:

$$y(\tilde{x}) = \hat{\beta} + \tilde{r}^T(\tilde{x}) R^{-1}(\tilde{y}_s - \tilde{F}\hat{\beta}) \quad (12)$$

where $\tilde{r}^T(\tilde{x})$ is defined in Equation (6). Equation (12) comprises the metamodel developed by the Kriging method.

In this project codes based on the OSLH and the Kriging methods are employed for generating all of the metamodels. The computational capability of generating metamodels is utilized in two areas. First, metamodels are developed for enriching the response matrix of the measurements from a limited amount of test data. Responses can be generated for points on the ship where test data were not originally collected. Metamodels are also employed during the probabilistic model updating process and in the assessment of the error estimation.

2.2 Principal Component Analysis (PCA)

Principal components are computed for the response matrix from the test and from the numerical model. Both matrices have the form:

$$[X] = \begin{bmatrix} x_1(t_1) & \cdots & x_1(t_n) \\ \vdots & \ddots & \vdots \\ x_m(t_1) & \cdots & x_m(t_n) \end{bmatrix} \quad (13)$$

where each row corresponds to a different location either on the model or on the physical system where responses are computed or measured, respectively; each column corresponds to a different time step. The PCA allows to convert the rime histories into "modal" type of information through a singular value decomposition. The time histories included in the response matrix include non-linear effects, such as yielding, interaction between the load and the flexible structure, etc. The response matrix [X] is written as:

$$[X] = [U][W][V]^T \quad (14)$$

where [U] is a matrix which contains "modal" type of information about the measurement locations in each column. [W] is a diagonal matrix which contains information about the energy associated with each mode placed in each column of [U]. $[V]^T$ is a matrix which contains time domain information about how the "modes" are synthesized in order to produce the time histories. Figure 1 summarizes the information which is contained in the principal components.

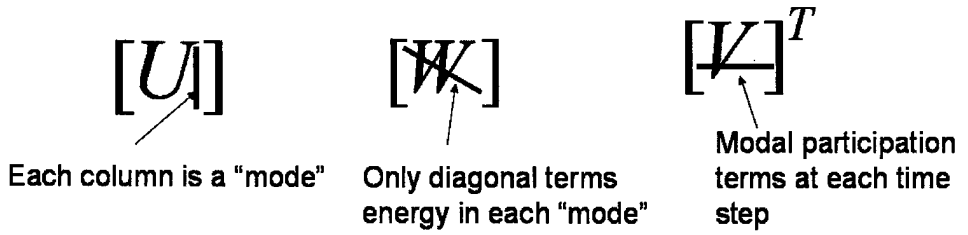

Figure 1. Information contained in principal components of a response matrix

Principal component analysis is useful for non-linear models for the same reason that modal properties are useful in linear dynamic systems for comparing analysis and test data. In linear structural dynamics, the structural modes are associated with resonant frequencies. In non-linear systems the interpretation of modal properties in general depends on the selection of the response data included in matrix [X]. The PCA provides a compact representation of the response for a non-linear model. Figure 2 presents the first four "modes" for one quarter of a simply supported plate with an impact load applied at the middle of the plate. It can be observed that the "modal" information contained in each one of the columns of the [U] matrix increases in complexity for higher modes and that each "mode" satisfies the physical boundary conditions.

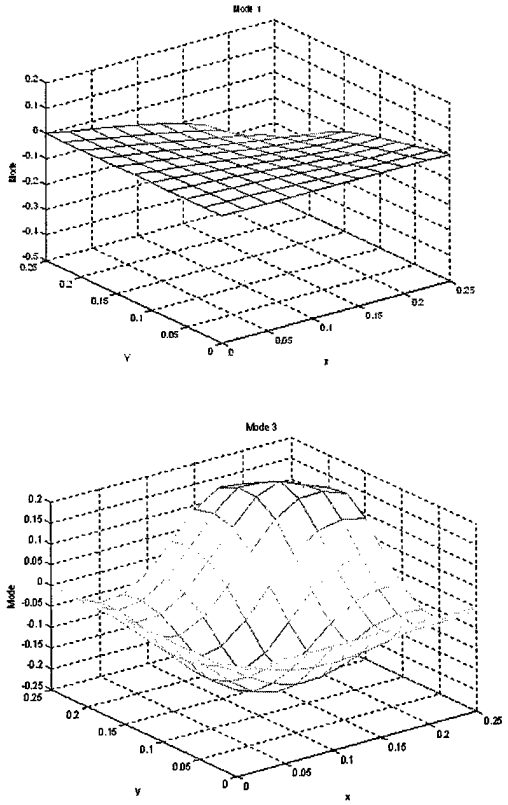

Figure 2. Example of PCA "modes" for the quarter of a simply supported plate due to an impact load applied at the middle of the plate

In order to perform the principal component decomposition, equation (14) is re-written as:

$$[X] = [\Phi \quad \Phi_\tau] \begin{bmatrix} D & 0 \\ 0 & 0 \end{bmatrix} \begin{bmatrix} \eta \\ \eta_\tau \end{bmatrix} \tag{15}$$

where $[W] = \begin{bmatrix} D & 0 \\ 0 & 0 \end{bmatrix}$, $[U] = [\Phi \quad \Phi_\tau]$, $[V]^T = \begin{bmatrix} \eta \\ \eta_\tau \end{bmatrix}$

The principal components decomposition is based on equation (15) and results in the following expression for [X]:

$$[X] = [\Phi][D][\eta] \tag{16}$$

Equation (16) constitutes the principal components decomposition of the response matrix either from the test or from the analysis. The matrices $[\Phi_\tau]$ and $[\eta_\tau]$ do not participate in the definition of matrix [X] since they are both multiplied with the zero entries of matrix [W], and therefore they are not considered in the definition of the principal components.

In this project a code has been developed for performing PCA analysis for a response matrix. The PCA code is employed for probabilistic model update and for error estimation. The corresponding results demonstrate the utilization of the PCA code.

2.3 Enrichment of test data

Since test data only at a limited number of locations may be available, a capability to essentially increase the number of rows in the response [X] matrix was developed. For each time step the physical information in a column of the test matrix is used along with the corresponding coordinates of the locations where the test data were collected, in order to generate metamodels for the measured data. The Kriging code is employed here for enriching the test data. The process is summarized in Figure 3:

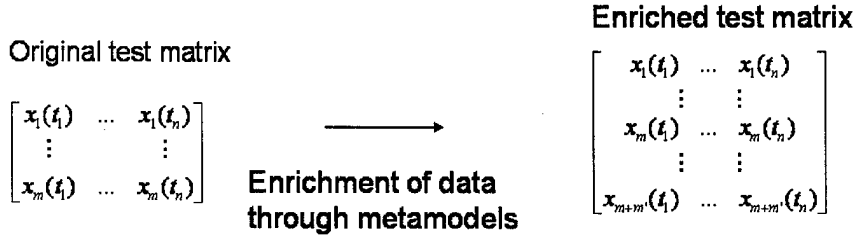

Figure 3. Process of enriching the test data

Results form two different applications are presented in order to validate the capability of enriching the test data. The first application is associated with a rectangular plate subjected at its center to an impact load of short duration. The finite element model of this plate has ~2,700 degrees of freedom (dof) and due to its relative small size, this model was utilized for the initial validation of all new developments. The duration of the impact load is selected in such a manner to represent typical durations from shock loads in naval applications. The finite element model for the plate is depicted in Figure 4 and the load time history is depicted in Figure 5. LS-DYNA is utilized for the analysis.

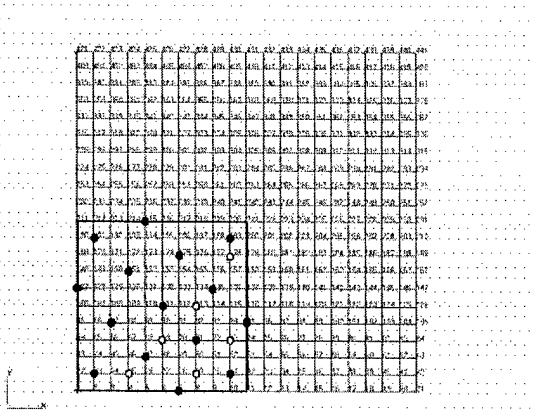

Figure 4. Finite element model for the plate utilized in the validation/demonstration.

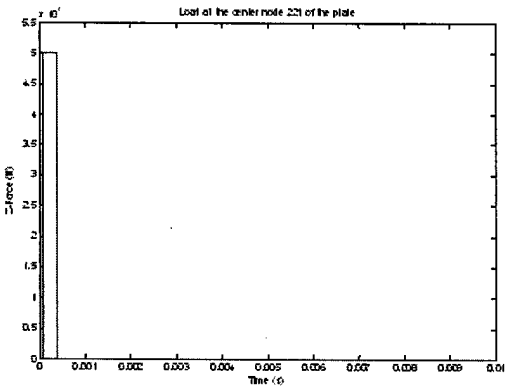

Figure 5. Time history of the load applied on the center of the plate.

The second application is associated with a section of a typical surface ship subjected to a load with time history similar to typical loads in underwater explosion applications. The finite element model for a typical ship is presented in Figure 6. LS-DYNA is employed again for performing the non-liner FEA analyses. Each finite element in the ship model has approximate main dimension of 1ft. The ship section is analyzed as part of the case study of this project. All the steps which were originally validated and demonstrated through the simple plate model are validated and demonstrated as well by the ship section model in a parallel effort. The ship section model and the corresponding loads were selected in collaboration with NN in order to make certain that the case study has Naval relevance. The ship section finite element model has ~55,000 dof. The model contains bottom frame members, stiffeners, bulkheads, and a double bottom structure.

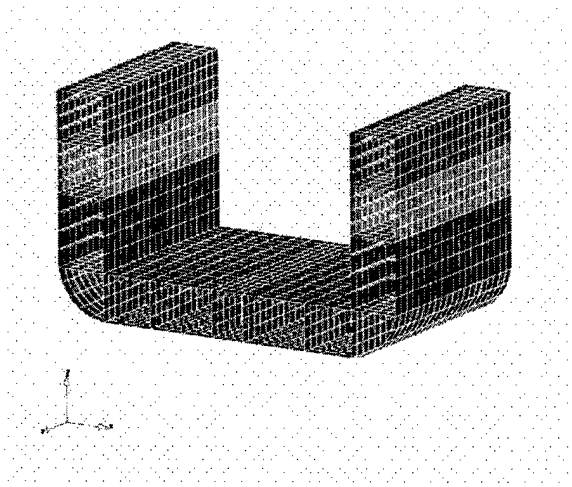

Figure 6. Typical ship model (left), and the section of the ship model (right) which is utilized in the case study

In order to validate and demonstrate how the enrichment of the test data process operates 15 points marked in Figure 4 with dark circles are used as sample points for developing metamodels for the response at the 6 points which are marked with plain circles in Figure 4. Analysis is performed by LS-DYNA. The time histories at the 15 sample points comprise the original response matrix. The Kriging code is used to generate the time histories for the response at the other 6 points and augment the original response matrix, thus generating the enriched response matrix. The time histories computed by the Kriging code are compared to the actual LS-DYNA results (Figure 7). Very good correlation is observed between the actual LS-DYNA results and the acceleration time histories created by the Kriging code for all 6 evaluation points. The correlation for two representative nodes is presented in Figure 7.

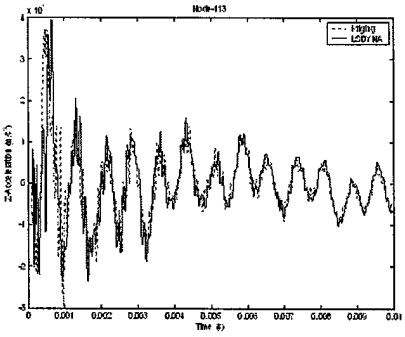

Figure 7. Time histories for the enriched response matrix computed by the Kriging code and compared to actual LS-DYNA results

A similar analysis is performed using the ship section (Figure 6). Since the induced velocity response at bulkheads is a primary parameter measured in a typical underwater explosion test, the normal velocity at the 12 nodes marked with dark circles in Figure 6 comprise the information at the sample points. Time histories for the induced velocity at the six points marked with the plain circles in Figure 6 are generated by the Kriging code from the information at the sample points. The time histories generated by the Kriging code and those computed by the actual LS-DYNA analysis are compared for all 6

evaluation points. Results for 3 evaluation points (one from each bulkhead) are presented in Figure 8.

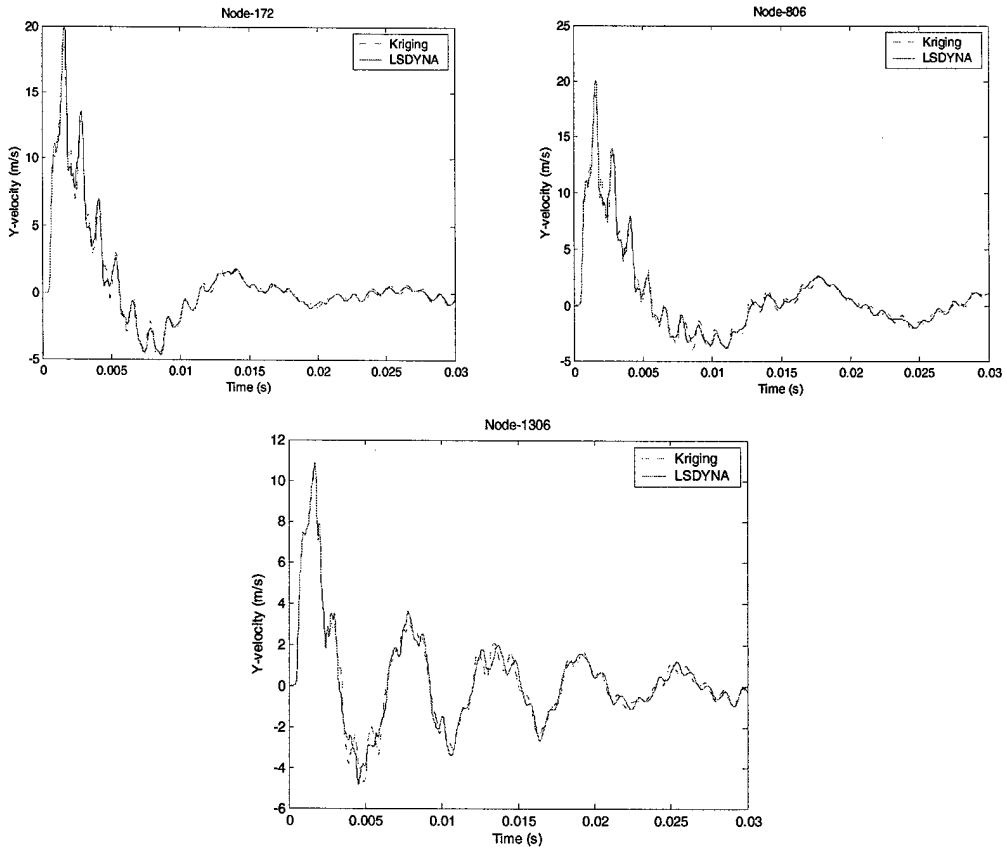

Figure 8. Time histories for the enriched response matrix computed by the Kriging code and compared to actual LS-DYNA results for the case study model

Very good correlation is observed for the velocities at all the points between the Kriging code and the actual LS-DYNA analysis. As a clarification, the LS-DYNA results at the evaluation points were not utilized when computing the response at the evaluation points through the Kriging code. Only the LS-DYNA results at the sample points were employed for this purpose in both applications.

In order to further demonstrate and validate the enrichment process, PCA is performed for a response matrix comprised exclusively from LS-DYNA results and a response matrix comprised by LS_DYNA results for some points and by enriched data for other points. The plate presented in Figure 9 is utilized again

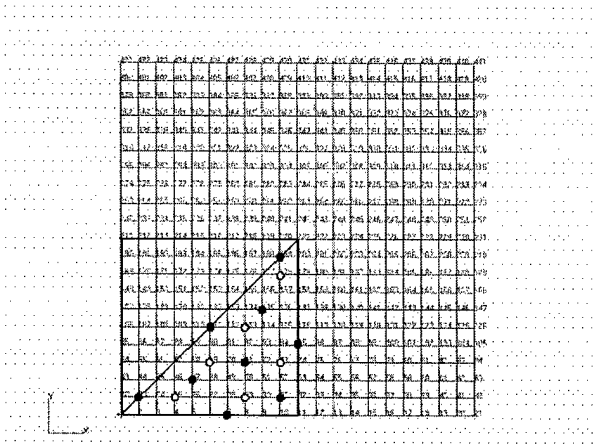

Figure 9. Sample points and evaluation points for used in PCA and Kriging code validation

In this case the LS-DYNA results at the 9 points marked with the dark circles along with the time histories computed by the Kriging method at the 6 points marked with the plain circles are used for defining the response matrix. The PCA is performed for the response matrix. The PCA results are compared with the PCA results computed for a response matrix which is comprised by all 15 (9+6) time histories computed by LS-DYNA. Since the same PCA results are generated for both response matrices, this indicates that the enrichment of the data is performed correctly. Using the PCA results, the vibration at the 6 points marked with the plain circles is also reconstructed and compared with the actual LS-DYNA vibration responses at these points (Figure 10).

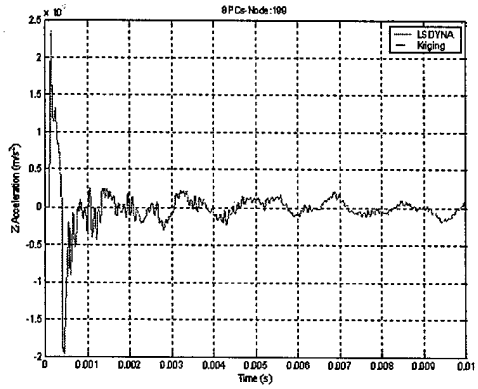

Figure 10. Reconstructed vibration from PCA when using the time histories from both LS-DYNA and from the Kriging method vs. the actual LS-DYNA vibration results

The good correlation between the reconstructed responses in Figure 10, demonstrates that the Kriging code provides good quality time histories and that the concept of enriching the test data response matrix works properly.

Similar PCA and vibration reconstruction from PCA results is performed for the ship section of the case study (Figure 6). The LS-DYNA response at the 12 points marked with dark circles and the Kriging results at the 6 points marked with plain circles in Figure 6 constitute one response matrix, and the corresponding results are labeled as

"Kriging" in the Figures. The LS-DYNA results at all 18 (12+6) points constitute a second response matrix. PCA are performed for both. The diagonal terms of matrix [D] (Equation 16), representing the energy in each PCA "mode", are presented in Figure 11 for both analyses.

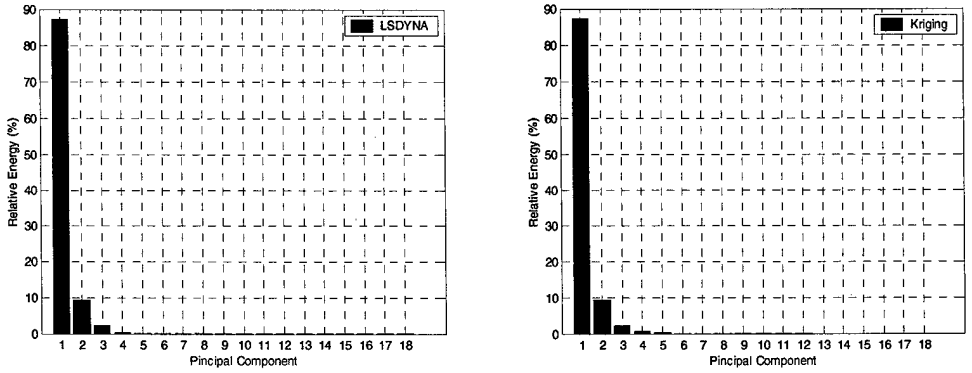

Figure 11. Diagonal terms of [D] matrix from PCA analyses

The reconstructed response from the principal components created by both PCA analyses are presented in Figure 12 for two of the nodes.

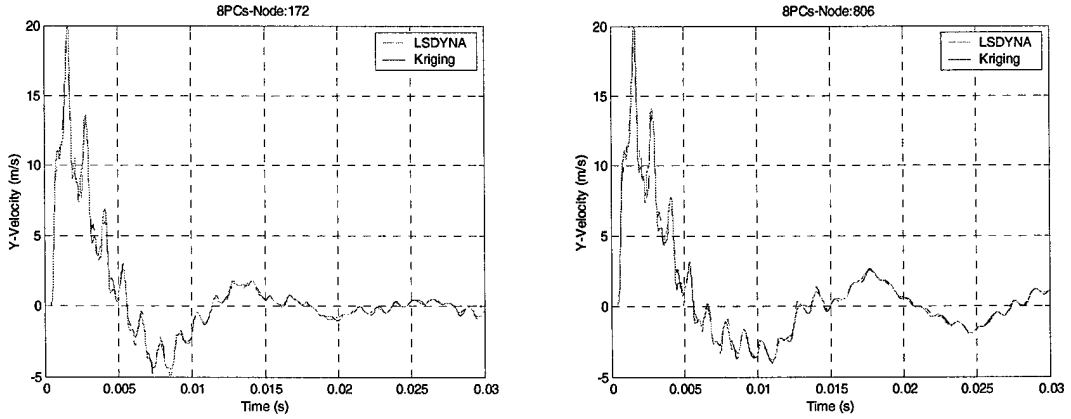

Figure 12. Reconstructed response from the PCA analyses

Very good correlation is observed between all the results produced from the PCA analysis based on all LS-DYNA results, and the PCA analysis which is based on some LS-DYNA results and some Kriging results. Thus, once again the test data enrichment process and the PCA development are validated through the case study results.

2.4 Probabilistic model updating

Model-to-test correlation metrics similar to the ones used in linear structural dynamics are established based on the principal components of the test and the response matrices. The following set of model-to-test correlation metrics are defined:

$$\Delta\Psi = {}^{o}\Phi^{T}\,\Phi - I \qquad (17\text{ a})$$

$$\Delta\nu = \eta\;{}^{o}\eta^{T} - I \qquad (17\text{ b})$$

$$\Delta\tilde{D} = {}^{0}D^{-1}\,[D - {}^{o}D] \qquad (17\text{ c})$$

the left superscript zero indicates variables from the analysis and variables without superscript originate from the principal components of the test matrix. The measures established by equations (17a – 17c) are generic. The cross orthogonality matrices on the right hand side of equations (17a) and (17b) are the directional cosine matrices between the respective spaces spanned by the principal vectors. The scaled differences of singular values in equation (17c) represent the differences in energy content for the corresponding principal components. The uncertainty of the system response is determined by considering the variation of the response as a function of the normalized model-to-test correlation matrices.

The variation in the correlation metrics between the test and analytical results is defined as:

$$\Delta\tilde{r} = \begin{Bmatrix} vec(\Delta\Psi) \\ vec(\Delta v) \\ diag(\Delta\tilde{D}) \end{Bmatrix} \tag{18}$$

where the symbols vec( ) and diag( ) in equation (18) represent respectively, a column-wise vectorization of a matrix and a vector formed by the diagonal terms of a matrix.

By considering uncertainty in the parameters γ of the numerical model, equation (16) becomes:

$$[X(\gamma)] = [\hat{\Phi}(\gamma)]\,[D(\gamma)]\,[\eta] \tag{19}$$

where the columns of $[\hat{\Phi}(\gamma)]$ and the diagonal entries of $[D(\gamma)]$ are evaluated from metamodels developed by the Kriging method. Equation (19) represents a fast-running model for the response predicted by the analytical model. Utilizing fast-running models is critical in performing the model updating and the error estimation for any practical finite element model.

A common approach for minimizing the error between model predictions and experimental data, while introducing statistical information into the process is through minimization of a Bayesian-type of objective function:

$$J = (\vec{X} - {}^{o}\vec{X}(\gamma))\,[S_{XX}]^{-1}\,(\vec{X} - {}^{o}\vec{X}(\gamma))^{T} + (\gamma_o - \gamma)\,[S_{\gamma\gamma}]\,(\gamma_o - \gamma)^{T} \tag{20}$$

where $[S_{XX}]$ is the covariance matrix of measurement uncertainty, $[S_{\gamma\gamma}]$ is the covariance matrix of parametric uncertainty in the model, γ_o is the vector of the original parameters, γ is the updated vector of parameters, $\vec{X}$ is the vectorized measured time history, and ${}^{o}\vec{X}(\gamma)$ is the vectorized time history from the simulation as it is evaluated from equation (19). The covariance matrices $[S_{XX}]$ and $[S_{\gamma\gamma}]$ embody the a priori knowledge and beliefs regarding the errors in the measurements and the uncertainty in the parameters of the numerical model. The corresponding Fisher information matrices, $[F_{XX}]$ and $[F_{\gamma\gamma}]$ are the pseudo-inverse of $[S_{XX}]$ and $[S_{\gamma\gamma}]$, respectively. The covariance matrices act as weighting factors placing more importance on parameters associated with higher levels of certainty. The first term in the functional defined by Equation (20) minimizes the difference between the test data and the numerical results. The second term in Equation (20) imposes a requirement for a minimal possible change from the original numerical model during the model update process. The latter requirement contributes to the uniqueness of the solution from the optimization process.

Once the new parameter estimates are derived, the parameter covariance matrix $[S_{\gamma\gamma}]$ is updated through the first order Bayesian method:

$$[S^*_{\gamma\gamma}] = \left[[S_{\gamma\gamma}]^{-1} + [T_{X\gamma}]^T [S_{XX}]^{-1} [T_{X\gamma}]\right]^{-1} \quad (21)$$

where $[S^*_{\gamma\gamma}]$ is the revised covariance matrix of the parameter error, and $[T_{X\gamma}]$ is the sensitivity matrix. The updated pseudo-inverse matrix $[F^*_{\gamma\gamma}]$ is evaluated as:

$$[F^*_{\gamma\gamma}] = [F_{\gamma\gamma}] + [T_{X\gamma}]^T [F_{XX}] [T_{X\gamma}] \quad (22)$$

An optimization code has been developed based on Equations (20), (21), and (22) and is used for updating the simulation model. This updating process takes into account the confidence in the test data and the uncertainties in the numerical model. Thus, the updated numerical model correlates the best to the test data in a probabilistic sense. It is essential to update the model first in a probabilistic sense before employing it for analyses which include error estimation in the prediction in order to improve the confidence in the numerical results.

In order to validate and demonstrate the model update process the plate model presented in Figure 9 is utilized. Concentrated masses equaling the 35% of the total mass of the plate are distributed over the plate. The magnitude of the load, the yielding stress, and the values of the distributed masses were perturbed from the configuration that represents the "test" data. Table 1 summarizes the values of the variables assigned to the configuration representing the "test" data, the original numerical model, and the standard deviation assigned to each one of the variables in order to incorporate the uncertainty of the numerical model in the computations.

	"Test"	Original Model	Sigma
Yielding strength	1.95E8 N/m^2	3.90E8 N/m^2	0.975E8 N/m^2
Concentrated mass	0.40 Kg	0.15 Kg	0.06 Kg
Magnitude of load	5.0E4 N	4.0E4 N	0.5E4 N

Table 1. Summary of values for variables with uncertainty in plate impact model

For the three points identified in Figure 13, the "test" data, the results corresponding to starting point for the model update process, and the results corresponding to the update model are presented in Figure 14. As it can be observed, the perturbation which was introduced in the model resulted in a large initial difference between the "test" data and the starting point of the model update process. However, after the model has been updated the "test" data and the results for the updated model correlate well.

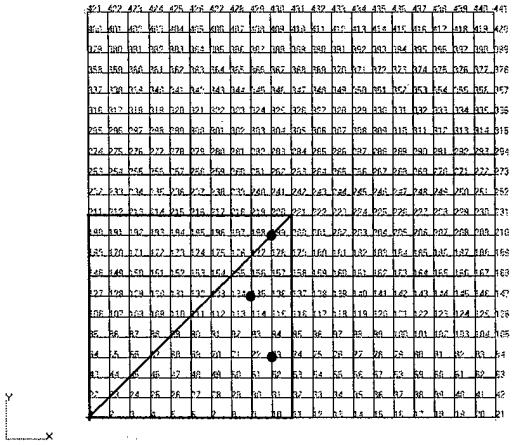

Figure 13. Three points for which results are presented before and after the model update process

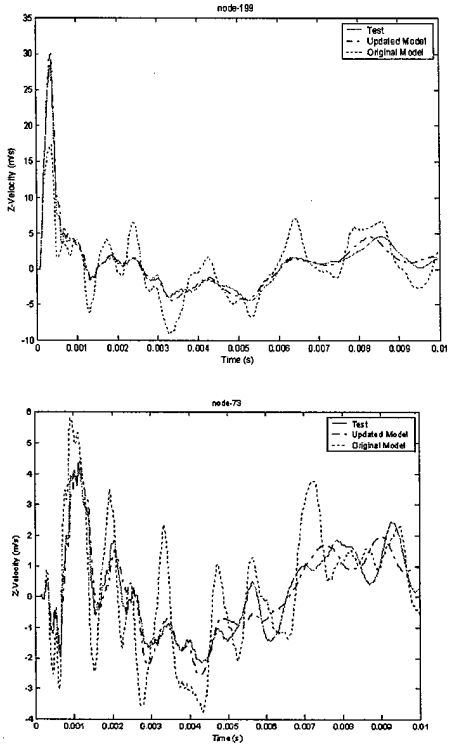

Figure 14. Response time histories for the "test" data, the model used as starting point in the model updating process and the finally updated model

Initially only the fast running model (Equation 19) was utilized during the model update process. Although the starting point for the model update process differed significantly from the "test" data, the updated model correlated well with the "test" data. This demonstrates that the probabilistic model updating process can handle large initial differences between the numerical model and the test data, while accounting for the uncertainty in the test and in the numerical model. A different scale is used for each one

of the three plots in Figure 14 since points closest to the impact location exhibit higher response.

The model update procedure was performed for a second time. The actual LS-DYNA code was executed every time that the model updating program required a new evaluation of the structural response. The final results for the updated model also matched the "test" data during the second model update analysis. However, a significant time reduction was achieved when using the fast running model as it can be observed from the cpu time comparison presented in Table 2.

	Run Time
LS-DYNA	~11 hours
Fast running model	~12 minutes

Table 2. cpu time comparison between model update based on LS-DYNA and model update based on a fast running model

The results demonstrate that the model update code operates correctly, that the Kriging code works properly when generating the fast running model, and that significant time savings can be realized when using the fast running model. Utilizing a fast running model in the model update process is crucial since the large LS-DYNA models used in ship applications would otherwise make the model update process infeasible.

2.5 Error Estimation

Once the numerical model has been updated, the fast running model based on Equation 19 and the principal component matrices $[D(\gamma)]$ and $[\eta(\gamma)]$ computed at the state of the updated model are employed for assessing the standard deviation in the response. Due to the small cpu time requirements of the fast running models a Monte Carlo simulation is performed in order to generate information about the standard deviation of the response from the uncertainty in the parameters of the model. The expected standard deviation in the response is computed for the updated model of the plate presented in the previous Section (Figure 14). Results for the velocity time histories from the "test" data, the original numerical model, the updated numerical model, and + or – two standard deviations from the updated model are presented in Figure 15. In this error estimation computations the standard deviation in the parameters with uncertainty was obtained from Table 1. The standard deviation of the response depends on the uncertainty considered in the parameters of the numerical model.

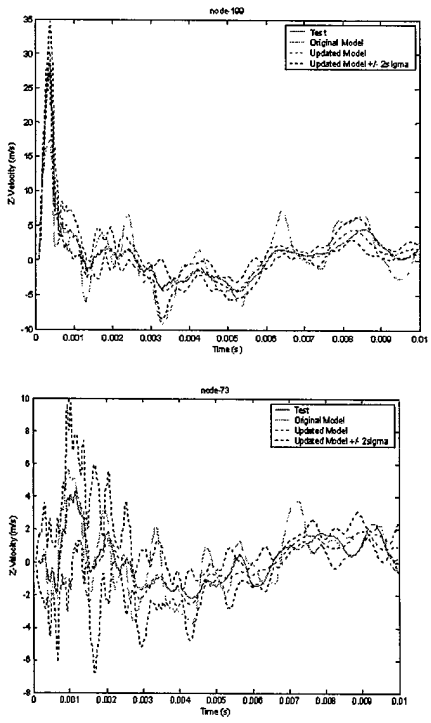

Figure 15. Response time histories for the "test' data, the starting model in the model update process, the updated model, and the + or – two standard deviations

Due to the intentionally large difference between the starting point for the model update process and the "test' data, the line which corresponds to the original model is often beyond the + or – two standard deviations. However, the difference between the updated model and the "test" data is almost exclusively within the + or – two standard deviations. The total run time for the error estimation was of the order of 1 cpu min on a Pentium 4 PC.

2.6 Case study

It is important to demonstrate that the new developments can handle the probabilistic model update and the error estimation with finite element models that contain a large number of dof, and that they can interact with commercial finite element codes. These capabilities are demonstrated through the case studies. The probabilistic model update and the error estimation capabilities presented in Sections 2.4 and 2.5 were applied on two different models. First, The model of the ship section presented in Figure 6 is used for validating and showcasing the developed capabilities on a model significantly larger and more demanding than the simple plate model (Figure 13) which was utilized during the development stages of the model update and error estimation process. A real application from an UNDEX test of a barge and the corresponding ABAQUS model were provided by NN and utilized to validate the new developments of this SBIR project. This barge application was not part of the original scope of the project. However, an extra effort was made by MES in order to demonstrate that the new developments work for real applications of Naval interests.

2.6.1. Probabilistic model update and error estimation for a hull section of a generic ship

The section of the ship hull used in this analysis is depicted in Figure 6. The velocities at the points on the longitudinal bulkheads which are identified in Figure 6 are considered in the model update process. The distribution of concentrated masses supported by the deck structure, and the magnitude of the impact load applied at the bottom structure are considered as the parameters with uncertainty. Table 3 summarizes the values that these parameters acquire for the "test" configuration, for the starting point of the model update process, and for the standard deviation considered in the variables.

	Loading (N)	**Mass (Kg)**
Test	7.5E6	3750
Original model	1.5E7	4125
Standard deviation	1.125E6	960.5

Table 3. Summary of values for variables with uncertainty in the ship hull analysis

The value of the load was selected high enough in order to introduce yielding in the longitudinal bulkheads. Figure 16 presents results for three points, one on each longitudinal bulkhead (Figure 6). For each point the results from the "test" data, from the configuration before the model update, from the updated model, and from + or – two standard deviations away from the updated model are presented.

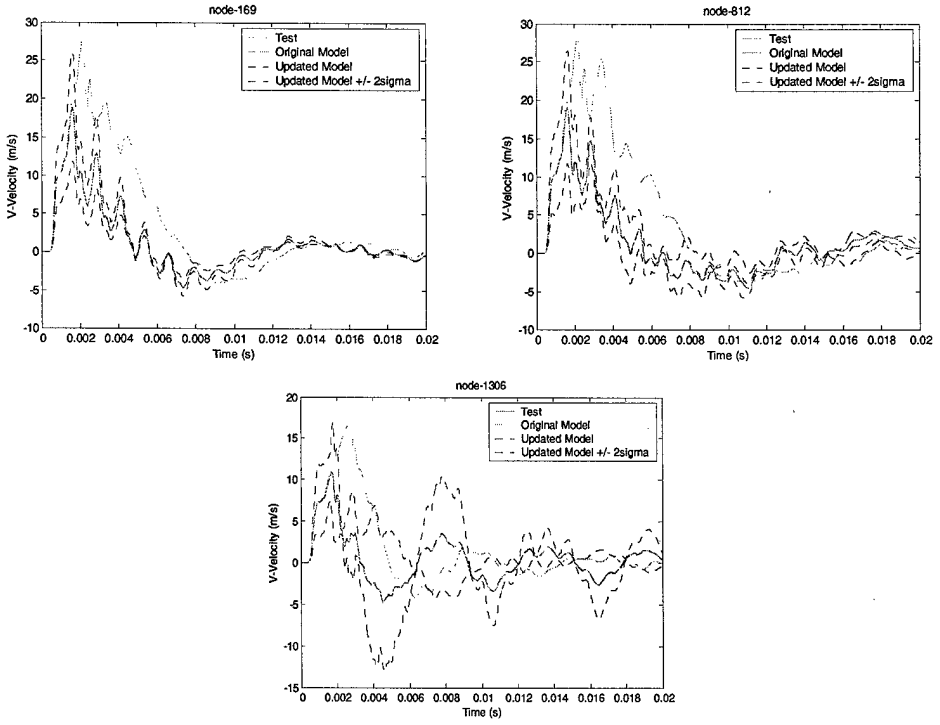

Figure 16. Initial difference between "test" (red line) and numerical model (blue line) for configuration used in the case study

As it can be observed the results from the original model (which comprises the starting point for the model updating process) differ significantly from the "test" results. This was done intentionally in order to demonstrate that the model update process works properly in adjusting the model in order to match the test data. The updated model matches the "test" data well, and the difference between the updated model and the test data is smaller than the two standard deviations margin which is also plotted in the Figures. In order to place the cpu requirements of the model update and of the error estimation process into prospective, a single complete LS-DYNA simulation for the section of the ship hull requires ~3 cpu hours. Once the fast running model has been generated, the probabilistic model update process requires ~25 cpu min, and the error estimation process requires ~6 cpu min on a Pentium III PC. Thus, the fast running models which are based on PCA make these analyses feasible for large finite element models.

2.6.2. Probabilistic model update and error estimation for a barge

The model of a barge in ABAQUS was provided by Jay Warren of NN. A picture of the barge is presented in Figure 17 [11]. The ABAQUS model contained both structural elements and fluid elements. The finite element model contains 4,934 structural elements and 74,560 fluid elements. The complete finite element model is depicted in Figure 18, and the structural portion of the finite element model in Figure 19. The charge was prescribed as a high pressure load applied on the fluid domain. The time history of the charge is defined according to Figure 20, and it is based on a simplified empirical model [12].

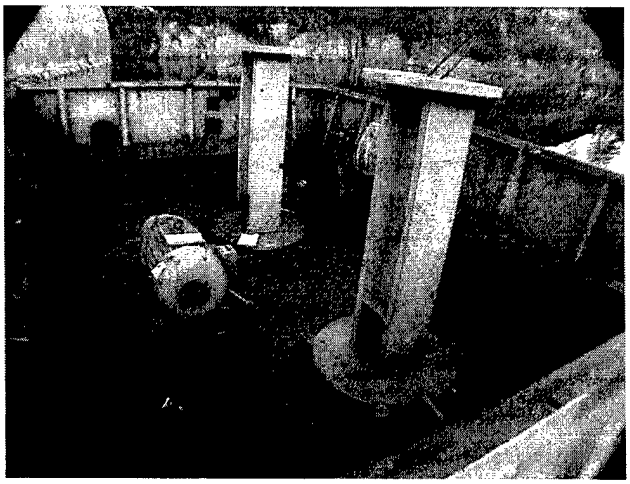

Figure 17. Barge for which vibration measurements are available [11]

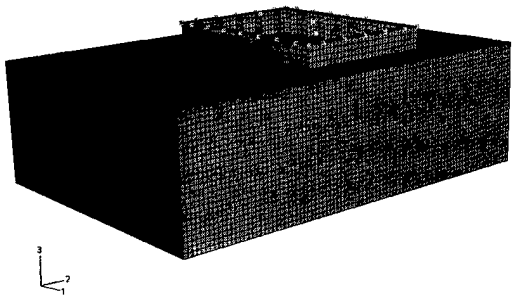

Figure 18. Complete FEA ABAQUS model with fluid and structural elements

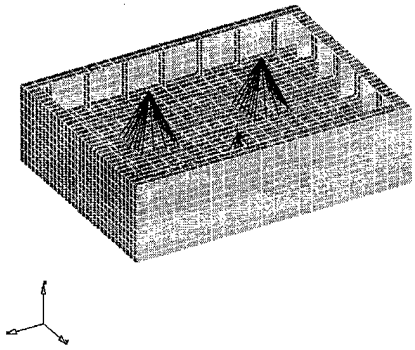

Figure 19. FEA ABAQUS model for the barge

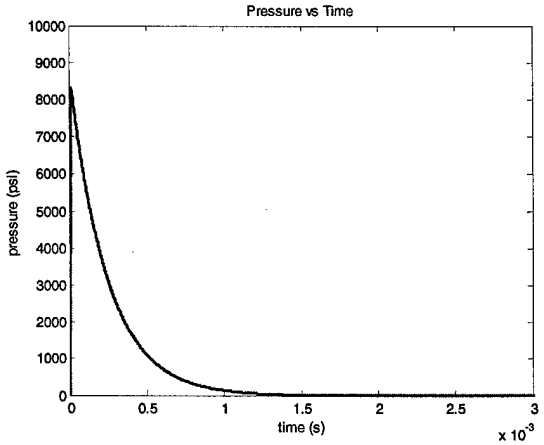

Figure 20. Definition of the load from the charge based on [12]

A velocity measurement from an UNDEX test was provided for a single location placed on the charge side and close to the centerline [11]. The configuration for which the test was performed targeted the collection of data associated with the performance of new mounts used to attach the two large masses to the deck structure. The only available velocity measurement corresponded to a single reference velocity measurement taken during the test. The peak value for the load and the location of the measurement point comprised the random variables in the probabilistic model update and the error estimation analyses. Based on a suggestion by Greg Harris (NSWC/IHD), the difference between

the shock spectra associated with the measured and the computed time histories of the velocity, comprised the correlation measurable in this case. Thus the objective function (Equation (20)) was modified to include the difference in the frequency spectra rather than the difference between the time histories. The fast running model represented by equation (19) was still used to compute the time histories of the velocity during the model update and the error estimation computations, but every time the velocity time history was processed in order to compute the corresponding shock spectrum. The velocity time history prescribed the base excitation for a single dof system with natural frequency "f", and the maximum value of the velocity induced on the single dof system was computed. Thus, the shock spectrum of maximum induced velocity vs. the natural frequency of the single dof system is generated.

Figure 21 presents the area within which the measurement location was considered to vary. The measurement location was considered as one of the parameters with uncertainty because there was no exact information about the location of the measurement point. In Figure 21 the area within which the measurement point is allowed to vary is highlighted. The velocity values computed at the nodes of the finite element model were interpolated based on the distance of the measurement point under consideration from the nodes. Then the corresponding velocity time history was used to generate the shock spectrum. The transverse and the longitudinal locations of the measurement point comprised the random variables expressing the uncertainty in the location of the point. The probabilistic model update analysis was performed first. The standard deviations for the three random variables considered in the analysis are summarized in Table 4. Once the model update was completed, the error estimation analysis was performed. The run time for the model update process was 14 cpu min on a Pentium 4 PC, and the run time for the error estimation was 6 cpu min on a Pentium 4 PC. All the results are summarized in Figure 22.

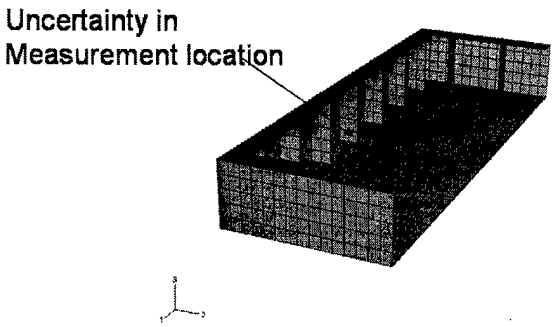

Figure 21. Uncertainty in the measurement location

Random variables	Sigma from updated values
Peak value of load	1284.0207 psi
longitudinal location	3.0 inch
transverse location	4.5 inch

Table 4. Summary of the standard deviations for the random variables considered in the barge analysis

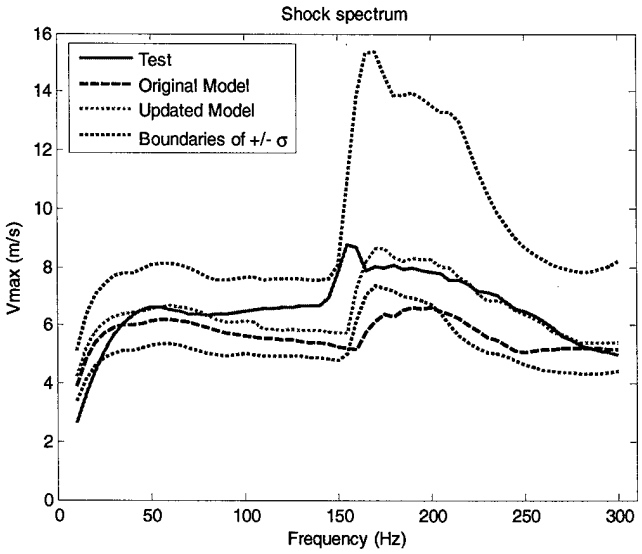

Figure 22. Results for shock spectra

The shock spectrum for the updated model matches much better the test data than the original numerical results. The boundaries associated with + or – one standard deviation are also presented in Figure 22. It can be observed that the response spectrum from the original model for certain frequencies is outside the error bounds associated with one standard deviation in the results. The test data and the numerical model fall within the + or – one standard deviation region for all frequencies.

This case study demonstrates that the codes developed for probabilistic model update and for error estimation can work with real models used in UNDEX simulations, and that they can produce meaningful results for real applications.

3. Potential developments during the Phase II effort

The main objective for the Phase II effort will be to further develop the capabilities of the probabilistic model update and the error estimation process in order to ensure their applicability in full scale naval ship applications. Further validation of the new methods should also be pursued. The following tasks can be performed: (this list has been developed through interactions with NN and NSWC/IHD)

- Investigate if the Principal Components can be extracted from analyses other than a complete UNDEX analysis. This capability will expedite the probabilistic model update process and the error estimation when using full scale ship models. It will allow developing the fast running models without performing time consuming UNDEX simulations but rather less time consuming analyses instead.

- Develop a variable screening process which will permit to limit the required number of simulations at sample points when developing the fast running models.

- Establish a correlation metric between the test data and the numerical results based on whether the test data can be recognized as a member of the family of the numerical solutions when considering the uncertainties in the numerical model.

- Apply the probabilistic model update and the error estimation processes to an automotive crash simulation for which both test data and numerical models are available.

- Work with NSWC/IHD in order to utilize the new processes developed by this project during the correlation phase between the numerical model and the test data of their joint project with the German Navy. A letter from NSWC/IHD stating this collaboration with MES under a Phase II contract, and endorsing the work and the proposal from MES is attached.

- Work on HMMWV applications where the vehicle structure is subjected to the blast load from a mine or an explosive device.

- Develop an interface of the probabilistic model update and error estimation processes and the LMS/Virtual Lab program. This development will accommodate commercialization of this technology beyond the Naval applications.

DEPARTMENT OF THE NAVY
INDIAN HEAD DIVISION
NAVAL SURFACE WARFARE CENTER
101 STRAUSS AVE
INDIAN HEAD, MD 20640-5035

3900
Ser 440/180
08 Oct 2004

From: Commander, Indian Head Division, Naval Surface Warfare Center
To: Office of Naval Research, Attn: Dr. Roshdy S. Barsoum, (Code 334), Ballston Center Tower One, 800 North Quincy Street, Arlington, VA 22217

Subj: ENDORSEMENT OF PHASE II SBIR FOR PROBABILISTIC ERROR ESTIMATION IN MODEL BASED PREDICTIONS

1. The Naval Surface Warfare Center Indian Head Division (NSWC/IHD) works on the Navy's mission-critical areas such as: energetics research, weapons product development, detonation science, underwater warheads, ordnance test and evaluation, and weapon simulations. Specifically in the area of accurate modeling and simulation of underwater explosion damage to naval structures, IHD/NSWC has developed the DYSMAS code. This development is based on coupling of a hydrocode with a simulation model of the target structure within a parallel computing environment. In order to validate and demonstrate the simulation capabilities of the DYSMAS code IHD/NSWC is currently performing jointly with the German Navy a full-scale simulation and test program for a surface ship. The scope of this work is to model and test eight different configurations and compare results between simulation and test.

2. During the past five months Nick Vlahopoulos of Michigan Engineering Services, LLC (MES) has interacted with IHD/NSWC and has communicated results of the work that MES has performed under the Phase I SBIR contract N00014-04-M-0124 titled "Probabilistic error estimation in model based predictions." The technology that MES is developing is practical, technically sound, and promising for combining results from existing or commercial non-linear finite element codes with information from test in order to update the numerical models under uncertainty and provide an error estimation capability along with the numerical predictions. The value of their developments has been demonstrated through case studies which utilize large size finite element models and test data from Naval applications.

This report was prepared by Nickolas Vlahopoulos, nv@miengsrv.com , phone # 734-355-0084.

1. NAVAL SEA SYSTEM COMMAND, "Shock Design Criteria for Surface Ships," NAVSEA 0908-LP-000-3010, Colts Neck, NJ, 1995.
2. Kammer, D.C., "Sensor Placement for On-orbit Model Identification and Correlation of Large Space Structures," J. Guid. Control Dyn., Vol.14, pp. 251-259, 1991.
3. Kammer, D.C., "Effect of Model Error on Sensor Placement for On-orbit Modal Identification of Large Space Structures," J. Guid. Control Dyn., Vol.15, pp. 334-341, 1921.
4. Horta, L. G., Lyle, K. H., Lessard, W. B., "Evaluation of a Singular Value Decomposition Approach for Impact Dynamic Data Correlation," NASA/TM-2003-212657, NASA Langley Research Center, Hampton, Virginia.
5. Cressie, N., "Spatial Predication and Ordinary Kriging," Mathematical Geology, Vol.20, No.4, pp.405-421, 1988.
6. Sacks, J., Welch, W.J., Mitchell, J.J., and Wynn, H.P., "Design and Analysis of Computer Experiments," Statistical Science, Vol.4, No.4, pp.409-435, 1989.
7. Anderson, M.C., Hasselman, T.K., and Crawford, J.E., "A Toolbox for Validation of Nonlinear Finite Element Methods," 7th International LS-DYNA Users Conference, Minneapolis, MN, 2000.
8. Anderson, M.C., Gan, W., and Hasselman, T.K., "Statistical Analysis of Modeling Uncertainty and Predictive Accuracy for Nonlinear Finite Element Methods," Proceedings of the 7th Shock and Vibration Symposium, Minneapolis, MN, 1998.
9. J. Wang, N. Vlahopoulos, Z. P. Mourelatos, O. Ebrat, K. Vaidyanathan, "Probabilistic and Sensitivity Analyses for the Performance Characteristics of the Main Bearings in an Operating Engine due to Variability in Bearing Properties," accepted by *International Journal of Vehicle Design*.
10. J. Wang, N. Vlahopoulos, Z. P. Mourelatos, O. Ebrat, K. Vaidyanathan, "Probabilistic Analysis for the Performance of Engine Bearings due to Variability in Bearing Properties," SAE Noise and Vibration Conference, Traverse City, May 2003, SAE Paper 2003-01-1733.

11. "Report No: 1108, Heavyweight high impact shock testing of vibracon mounts," HI-TEST Laboratories INC., Government contract N00167-01-D-0017, DO 0005, February 2003.
12. T. L. Geers, Y. S. Shin, "Response of Marine Structures to Underwater Explosions," Short Course Lectures offered at Newport News, August 2002.